Knowledge-based Engineering and Sciences (2025), **6**, (3), 1–26
doi:10.51526/kbes.2025.6.3.1-26

RESEARCH PAPER

Seismic Stability Analysis of Slopes using Limit Equilibrium and Finite Element Method

Izzeldeen Alhashlamoun, Ehab K. Alfuqaha, Abdirahman Jamal Ahmed,* and Ibrahim Altarouti

Civil and Environmental Engineering Department, King Fahd University of Petroleum and Minerals, Saudi Arabia
*Corresponding author. Email: amaanjamaal19@gmail.com

(Received 08 November 2025; revised 01 December 2025; accepted 07 December 2025; first published online 31 December 2025)

Abstract

Seismic slope instability poses a major hazard in earthquake-prone regions, where ground shaking can cause sudden slope failures resulting in severe damage and loss of life. Reliable assessment of seismic slope performance is therefore essential for geotechnical design. This study compares the Limit Equilibrium Method (LEM) and the Finite Element Method (FEM) in evaluating slope stability under pseudo-static and dynamic loading. The analysis investigates the effects of horizontal (k_h) and vertical (k_v) seismic coefficients, soil constitutive models, mesh refinement, and earthquake loading types on the Factor of Safety (FoS). Pseudo-static results show a clear reduction in stability with increasing seismic intensity. As the horizontal coefficient increases from $k_h = 0.0$ to $k_h = 0.20$, the FoS decreases from 1.706 to 0.945 in LEM and from 2.018 to 1.123 in FEM. Vertical acceleration further reduces FoS, especially when $k_v \approx 0.75k_h$. FEM consistently predicts higher stability than LEM, typically by $17 - 19\%$, due to its ability to model stress redistribution and deformation compatibility. Analyses of constitutive models and mesh refinement indicate close agreement between Mohr-Coulomb and Hardening Soil Small models, with differences generally within $1 - 3\%$, while finer meshes reduce FoS by $2 - 7\%$ due to improved strain localization. Dynamic simulations show that time-history loading produces slightly higher FoS than pseudo-static analysis, whereas harmonic cyclic loading yields the lowest stability. These results highlight the importance of advanced numerical modeling and realistic seismic input in achieving reliable assessments of seismic slope stability.

Keywords: Seismic slope stability; Earthquake loading; Slope safety; Numerical modeling; Stress redistribution; Dynamic analysis.

1. Introduciton

Seismic slope instability is one of the most hazardous phenomena in seismically active regions because it can trigger large-scale catastrophic landslides and cause severe damage to structures. Earthquakes can trigger sudden failure of slopes if they exert inertial forces greater than the resisting shearing strength of the ground or rock mass. Post-seismic surveys after a catastrophic earthquake such as the 2008 Wenchuan earthquake in China revealed that a large proportion of secondary disasters induced failure of slopes and led to casualties and destruction of structures. The seismic behavior of slopes is also an area of interest from the geological catastrophe risk reduction point of view, especially for high and steep slopes that exhibit more complex types of failure [1].

The seismic stability of slopes is a function of a combination of ground motion characteristics, slope geometry, ground conditions, and groundwater, all of which interact to control the potential

for failure. Among the primary factors identified in various studies are the ground motion parameters, including the peak ground acceleration (PGA), duration of shaking, and seismic wave frequency content. These directly or indirectly affect the driving forces acting on the slope and significantly influence the factor of safety (FoS) during an earthquake [2]. The studies show that higher PGA and longer shaking time relate to more displacement of the slope and reduce safety margins.

Apart from seismic loading, soil factors like cohesion, friction angle, modulus of elasticity, and damping ratio are also responsible for seismic slope stability. Soils that are more rigid have better resistance to deformation, whereas weak, clayey soils can experience strength degradation under cyclic loading, thereby decreasing the overall stability of the slope [3]. Furthermore, failure mechanisms like tensile–shear rupture are themselves dependent on the location and characteristics of the possible planes of fracture, and these are influenced by the soil type and seismic input energy.

Another significant factor is the existence of groundwater or a raised water tables that results in pore water pressure, thereby decreasing the effective stress and shear strength of the soil under seismic loading. This aspect severely degrades the stability of the slope, especially with horizontal seismic acceleration factors incorporated within the analysis [4]. Various studies have examined the effects of different factors or mechanisms on the stability of slopes. The factors include those mentioned earlier, such as PGA, cumulative damage from repeated earthquakes, vertical components of seismic motion, and post-earthquake failures. These factors collectively contribute to the destabilization of slopes and should be taken into account in stability assessments. For instance, cumulative damage from repeated earthquakes can progressively weaken slope materials, amplify PGA, and reduce natural frequency, leading to delayed or secondary failures. Vertical seismic components can induce trampoline effects and tensile failure, amplifying displacement beyond that caused by horizontal shaking alone. Furthermore, post-earthquake failures can occur due to accumulated plastic strains, slope cracking, and pore pressure buildup, resulting in progressive displacement even after shaking ends. These delayed or secondary failures highlight the need for robust analytical approaches that can capture both immediate and post-seismic slope responses. A concise summary of these influencing factors, their effects on slope stability, and relevant case studies is presented in Table 1 to provide a clearer understanding of their interrelationships and practical implications.

Huang and Peng [9] emphasized the significance of permanent displacement as a deformation-based measure that effectively captures the influence of dynamic pore water pressure and soil non-linearity. In their study, they proposed an approach that integrates the Limit Equilibrium Method (LEM) with the Finite Element Method (FEM), providing an accurate yet simplified framework for seismic slope stability analysis, validated through shaking table experiments. This combined methodology offers a more reliable basis for evaluating slope performance and designing reinforcement measures in earthquake-prone regions. Zhang [7] demonstrated that the upper portion of slopes is particularly prone to tensile failure under seismic loading, whereas the lower portion tends to fail in shear. This dual-mode failure mechanism complicates the identification of potential failure planes and necessitates advanced analytical approaches capable of capturing both behaviors. These findings underscore the critical need for robust and effective techniques in assessing slope stability within seismically active regions.

Recent studies have further advanced the understanding of seismic slope stability by systematically comparing analytical and numerical approaches. Yang et al. [10] proposed a two-dimensional slope stability analysis that integrates the finite element stress field with the limit equilibrium principle to determine the critical slip surface, demonstrating both high accuracy and computational efficiency. Similarly, Loukidis et al. [11] applied numerical limit analysis to assess seismically loaded slopes and reported strong consistency between the results of the FEM and the LEM, thereby validating the reliability of both approaches under pseudo-static conditions. Furthermore, Khan and Wang [12] conducted a comparative study of highway slopes using LEM and FEM and found that FEM produced slightly more conservative safety factors under dynamic loading, highlighting its superior

Table 1: *Summary of key factors and mechanisms affecting slope stability during and after earthquakes, with associated effects and representative case studies.*

Factor / Mechanism	Effect on Slope Stability	Case Study / Reference
Seismic loading (PGA, shaking duration)	Reduces FoS, increases displacement and slope destabilization.	Gyeongju Earthquake (South Korea): PGA up to 2g reduced FoS of previously stable slopes [5]
Cumulative damage from repeated earthquakes	Progressive weakening of slope materials, amplification of PGA, and reduction of natural frequency leading to delayed failure.	Xinmocun Landslide (China): Damage accumulation from multiple seismic events [6]
Vertical seismic components	Enhance trampoline effects and tensile failure, amplifying displacement beyond horizontal shaking alone.	Daguangbao Landslide (2008 Sichuan Earthquake): Vertical shaking induced significant instability [7]
Delayed or secondary failures (post-earthquake)	Occur due to accumulated plastic strains, slope cracking, pore pressure buildup, and progressive displacement after shaking ends.	Post-earthquake rainfall-induced failure in bedrock slopes (China); Seepage-induced liquefaction post-shaking [8]

capability to simulate stress redistribution and strain localization.

Several researchers have further developed hybrid or modified methods that combine the strengths of both LEM and FEM approaches. Acharya et al. [13] demonstrated that when correctly implemented, both techniques yield comparable results for slope stability if material parameters and boundary conditions are properly defined, highlighting FEM's ability to capture the plastic zones within the soil mass. Likewise, Baba et al. [14] applied both methods to a railway slope in the Moroccan Rif and found that FEM provided a more realistic representation of soil deformation and failure zones compared to LEM's simplified slip surface assumption. These comparative findings underscore the complementary nature of both techniques, where LEM offers efficiency and simplicity, while FEM ensures greater precision and predictive reliability for complex slope geometries.

Recent advancements have also explored probabilistic and dynamic perspectives to improve the predictive accuracy of seismic slope analyses. Zhou and Qin [15] presented a finite-element upper-bound analysis that integrates pseudo-dynamic effects, improving the prediction of seismic responses compared to the traditional pseudo-static assumption. This study highlights the evolution of seismic slope stability analysis toward more refined and realistic modeling frameworks, reinforcing the importance of this study's comparative approach between LEM and FEM in capturing true slope behavior under earthquake conditions.

Although numerous studies have addressed individual aspects of seismic slope stability, a significant gap persists in comprehensive comparative analyses that systematically evaluate classical and advanced numerical methods under varied seismic loading conditions. Most conventional approaches, including the quasi-static and pseudo-static LEM, simplify the representation of dynamic loading and neglect soil-structure interaction effects. In contrast, the FEM provides a more realistic assessment by incorporating nonlinear material behavior, progressive failure, and stress redistribution, but its

application under seismic conditions is still limited in comparative frameworks.

Therefore, this study aims to fill this gap by performing a detailed comparative evaluation of slope stability using both the LEM and the FEM under pseudo-static and dynamic conditions. The main objectives of this study are interconnected and collectively address the identified research gap. Specifically, this research seeks to quantify how variations in horizontal (kh) and vertical (kv) seismic coefficients influence slope stability under different seismic intensities. It further examines the effects of soil constitutive models and mesh refinement on the FoS, ensuring that both material behavior and numerical resolution are accurately represented. In addition, the study evaluates how the duration and nature of earthquake loading—whether time-history or harmonic cyclic—affect the predicted stability response. By integrating these aspects, the study aims to identify the combination of modeling parameters that produce the most realistic and reliable results. Overall, the findings are expected to enhance understanding of the differences between the LEM and FEM in assessing seismic slope performance, providing engineers with a clear basis for selecting appropriate analytical techniques in practical geotechnical applications.

2. Comparison Between the Pseudo-Static Analyses of LEM and FEM

2.1 Pseudo-Static Analysis

Pseudo-static analysis remains a widely used approach for evaluating seismic slope stability, where seismic forces are modeled as static vertical and horizontal accelerations (k_h and k_v). FEM and LEM both adopt this approach, but they diverge significantly in terms of their assumptions, computational depth, and accuracy of failure prediction.

Terzaghi [16] initially employed a pseudo-static method to study seismic stability against slope failure. This method involves a single, monotonically applied vertical and/or horizontal acceleration to simulate earthquake forces. Although the inclusion of vertical acceleration is theoretically possible in pseudo-static analysis, it is rarely implemented in practice, as explained below. The vertical and horizontal pseudo static forces F_b and F_y, respectively, act through the centroid of the sliding mass and are expressed in Equations (1) and (2), respectively.

$$F_h = \frac{a_h W}{g} = k_h\, W \tag{1}$$

$$F_v = \frac{a_v W}{g} = k_v\, W \tag{2}$$

In this approach, a_v and a_h represent the vertical and horizontal accelerations, respectively, while k_v and k_h are the corresponding dimensionless vertical and horizontal pseudo-static coefficients. The term W refers to the weight of the potential failure mass. The use of infinite slope analysis under these conditions offers the advantage of simplicity and provides a reasonable approximation for shallow slope failures, particularly for earthquake-induced shallow and disrupted landslides, which are common in the study area. Given the typically thin landslide mass involved in such failures, it is assumed that the groundwater table lies beneath the failure surface, eliminating the influence of pore water pressure on the sliding plane. In the case of an infinite slope model, where seismic loads (both horizontal and vertical) act through the centroid of the sliding mass, the FoS can be determined using Equation (3). Figure 1 presents the forces acting on a triangular soil wedge above a planar failure surface under pseudo-static slope stability conditions.

$$FoS = \frac{[(1 - k_v)\cos i - k_h \sin i]\tan \varnothing' + \frac{c'}{\gamma D_t}}{(1 - k_v)\sin i + k_h \cos i} \tag{3}$$

Where, Fos = Factor of safety, k_h = Horizontal seismic acceleration coefficient, k_v = Vertical seismic acceleration coefficient, i = Inclination angle of the slope, $\emptyset'$ = Effective internal friction angle

of the soil, c' = Effective cohesion of the soil, γ = Unit weight of the soil, D_t = Thickness or depth of the potential sliding mass, and tan φ' = Tangent of the effective internal friction angle.

$$\text{FoS} = \frac{\text{resisting force}}{\text{driving force}} = \frac{\text{CI}_{ab} + [(\text{W} - \text{F}_v)\cos\beta - \text{F}_h \sin\beta]\tan\emptyset}{(\text{W} - \text{F}_v)\sin\beta + \text{F}_h \cos\beta} \tag{4}$$

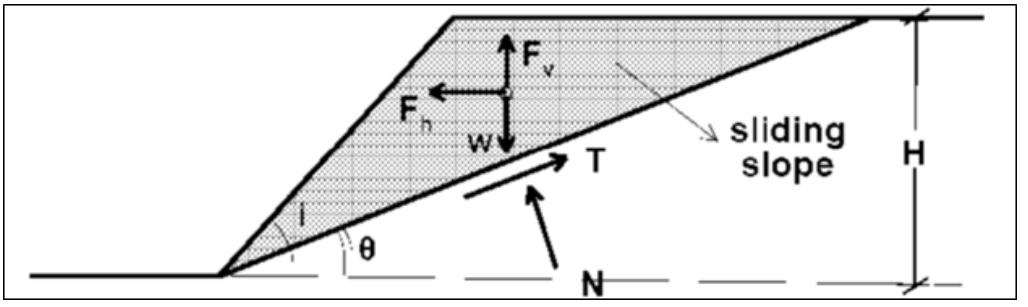

Figure 1: *Forces acting on triangular wedge of soil above planar failure surface in pseudo static slope stability analysis [18].*

In Equation 4, c and are ∅ parameters describing the Mohr-Coulomb shear strength parameters, defining shear strength along the failure plane, and l_{ab} is the failure surface length. In pseudo-static analysis, horizontal seismic force has an important role in lowering the FoS by concurrently augmenting driving forces and lowering resisting forces, especially when $\emptyset > 0$. Conversely, the vertical seismic force tends to have less effect on FoS, as it affects both driving and resisting forces in the same manner, augmenting or lessening them depending on the direction of vertical acceleration. Owing to this relatively less significant effect, vertical accelerations are usually ignored in pseudo-static slope stability analyses. The pseudo-static method may be successfully used to calculate FoS for different failure surface shapes, such as planar, circular, and noncircular failure surfaces. In addition, this method is also supported by most commonly used commercial limit equilibrium analysis computer codes, which most commonly provide provisions for conducting pseudo-static stability analysis [17].

2.2 Pseudo-Static Analysis of LEM vs FEM

LEM, as commonly implemented in tools like Slide2, relies on simplified assumptions about the slope geometry and failure surface. While its ease of use and speed make it suitable for preliminary design, it typically assumes rigid body motion and cannot model stress redistribution or deformation. As a result, it may yield conservative or inaccurate results under complex conditions. For example, in a comparative study of rock slope stability using seismic coefficients, it was found that LEM methods often produced less accurate or nonconservative factors of safety, especially in steep slopes or irregular geometries [18]. On the contrary, FEM allows a more accurate seismic response simulation by modeling soil-structure and stress-strain behavior. FEM can also include nonlinear material behavior and progressive failure as well as complex boundary conditions. FEM models based on the shear strength reduction (SSR) method have been found to show good agreement with field-observed deformation patterns and physical failure surfaces [15]. In another study, FEM generally produced more accurate slip surface predictions and accommodated progressive deformation, but LEM results were confined to FoS estimates only [19].

A particularly relevant comparison is found in a study of 431 slope cases using Slide2 (LEM) and Phase2 (FEM). It was observed that while static safety factors between both methods were close, pseudo-static analysis showed greater divergence as seismic coefficients increased. For $k_h > 0.1$ and

slope angles > 34°, FEM returned more realistic deformation patterns, and the MorgensternPrice method within LEM came closest to FEM results [20]. Furthermore, another study on volcanic rock slopes reported up to 78% difference in FoS values under pseudo-static conditions when comparing FEM and LEM. This significant variation was attributed to FEM's superior ability to model non-circular failure surfaces and accommodate highly fractured geological profiles [21]. However, LEM remains valuable for fast evaluations and is often used for screening or regional-scale seismic hazard assessments. Its reliability improves when advanced formulations like the Morgenstern-Price method are used, or when it is calibrated against FEM outputs. Still, as noted in early pseudo-static formulation studies, the inherent assumption of predefined slip surfaces and rigid-body motion limits its capability in dynamic conditions [22]. A detailed comparison between the LEM and FEM in pseudo-static slope stability analysis is summarized in Table 2.

Table 2: *Summary of comparison of pseudo-static analysis between LEM and FEM.*

Criteria	Limit Equilibrium Method	Finite Element Method	References
Failure Surface Assumption	Predefined (circular/non-circular); depends on chosen method such as Bishop, Janbu, etc.	Computed dynamically based on stress and deformation	[24]
Stress-Strain Modeling	Not considered; assumes rigid body behavior	Full stress-strain behavior modeled	[20]
Accuracy in Complex Geometries	Limited; may require manual refinement	High; can handle heterogeneity and irregular shapes	[22]
Prediction of Displacement	Not possible	Yes; displacement and deformation fields are included	[21]
Sensitivity to Material Nonlinearity	Low	High; can handle nonlinear material behavior	[23]
Computational Demand	Low; fast and easy for preliminary design	High; requires mesh refinement and more input parameters	[20]
(FoS) Reliability	Acceptable for basic conditions, but may deviate under high seismic loads	More consistent under variable seismic inputs	[22]

2.3 Pseudo Static Approach Limitations

Representation of the complicated, dynamic, and transient nature of earthquake shaking by a constant, single unidirectional pseudo-static acceleration is a very simplified practice. The shortcomings of the pseudo-static method had been realized at an early point. For example, Terzaghi [16] famously stated that "the idea it conveys with reference to earthquake effects on slopes is very inaccurate, to say the least," highlighting that a slope may still become unstable despite a calculated pseudo-static FoS greater than 1. More recent in-depth studies of past and recent earthquake-induced landslides have corroborated these concerns. These studies depict how pseudo-static analysis frequently is unable to represent the actual behavior of slopes subjected to dynamic earthquake loading, where causative failure mechanisms may include processes not addressed in this simplified practice. The major shortcomings of the pseudo-static method have long been reported in a variety of studies, such as [23-25]. These studies documented that pseudostatic analysis is likely not to predict the behavior of slopes accurately, especially in soils with a tendency to develop excess pore water pressures or when there is more than roughly 15% degradation in strength as a consequence of seismic vibrations. As illustrated in Table 3, there have been several cases where pseudo-static analysis gave values of

FoS significantly higher than 1 for several dams that later collapsed during earthquakes. These cases reveal that pseudo-static analysis is not able to reliably determine slope stability under conditions where weakening failure mechanisms like loss of strength or liquefaction are likely to develop.

Notwithstanding its limitations, the pseudo-static method is still employed as a fundamental screening device. Although it cannot make absolute stability predictions, it can provide a relative index of stability as an initial appraisal method in seismic slope stability assessments.

Table 3: *Results of pseudo-static analyses of earth dam that failed during earthquakes [8,28,29].*

Dam Name	k_h	FoS	Effect of Earthquakes
Sheffield	0.10	1.2	Complete failure
Lower San Fernando	0.15	1.3	Upstream slope failure
Upper San Fernando	0-15	2-2.5	Downstream shell, including crest slipped about 6 ft downstream
Tailings (Japan)	0.20	1.3	Failure of dam with release of tailings

3. The Effect of Change k_h and k_v and Comparison Between LEM and FEM

In pseudo-static analysis, seismic loads are simplified into constant k_h and k_v. These values simulate the effect of earthquake forces on a slope, and both LEM and FEM use them-but they interpret and respond to these loads very differently. When k_h increases, both LEM and FEM show a reduction in the FoS, but LEM tends to predict a sharper decline, especially in slopes with steep angles or weak soils. This is due to LEM's rigid-body assumption and simplified failure surface.

Additionally, k_v, though often omitted in simplified designs, becomes important in complex or highly seismic areas. LEM generally assumes k_v has minimal effect or applies it uniformly, which can misrepresent actual force distribution. FEM, on the other hand, can model vertical shaking more realistically. In a study comparing slope stability under combined k_h and k_v loads, FEM results reflected higher stress at the slope base and more accurate deformation paths, whereas LEM underestimated potential slip due to simplified force application [17].

Moreover, comparisons between observed failures and model predictions reveal that LEM may become nonconservative as seismic coefficients increase. In the case of the Upper San Fernando Dam, pseudo-static FEM closely matched observed deformation patterns during the 1971 earthquake, while LEM models using high k_h values overestimated safety and failed to capture displacement behavior [26]. Therefore, while both LEM and FEM reflect the sensitivity of slopes to seismic coefficients, FEM provides a more robust, realistic understanding of how k_h and k_v influence slope behavior especially under moderate to severe seismic loading.

3.1 The Effect of Change k_h and k_v: LEM Method

To better understand the influence of k_h and k_v on slope stability, Choudhury et al. [27] conducted a comprehensive pseudo-static analysis using the LEM. Their study evaluated the Dynamic Factor of Safety (DFS) for slopes under various combinations of soil friction angle (ϕ), slope angle (β), and seismic acceleration values. The results clearly demonstrate that as k_n and k_v increase, the DFS decreases, indicating a higher risk of failure.

Figures 2a–2d, adapted from Choudhury et al. [27], illustrate these relationships and provide a quantitative framework for assessing slope safety under different seismic conditions. Collectively, the figures demonstrate the impact of varying k_h and k_v on the DFS for slopes with different geometries and soil properties, analyzed using the LEM. Across all cases, an increase in the k_h results in a pronounced decline in DFS, reflecting a corresponding reduction in slope stability. This reduction is

further amplified by k_v, which decreases the DFS as it increases from 0 to $0.5k_v$ and subsequently to k_h.

Figures 2a, 2b, and 2c present results for slope angles of $\beta = 20°, 25°$, and $30°$, respectively, with soil friction angles (ϕ) ranging from $35°$ to $45°$. In all scenarios, higher ϕ values yield greater resistance to failure; however, even at $\phi = 45°$, the DFS declines markedly under higher seismic accelerations. Figure 2d isolates the influence of slope angle by maintaining $\phi = 40°$ and shows that steeper slopes (higher β) exhibit significantly greater susceptibility to seismic instability. Overall, the observed trends underscore that the LEM is highly sensitive to variations in seismic input parameters. Its inherent simplifications-particularly the assumption of a predefined failure surface and the neglect of deformation and progressive failure-may lead to an underestimation of seismic displacements and failure mechanisms that could be more accurately captured through advanced numerical approaches such as the FEM.

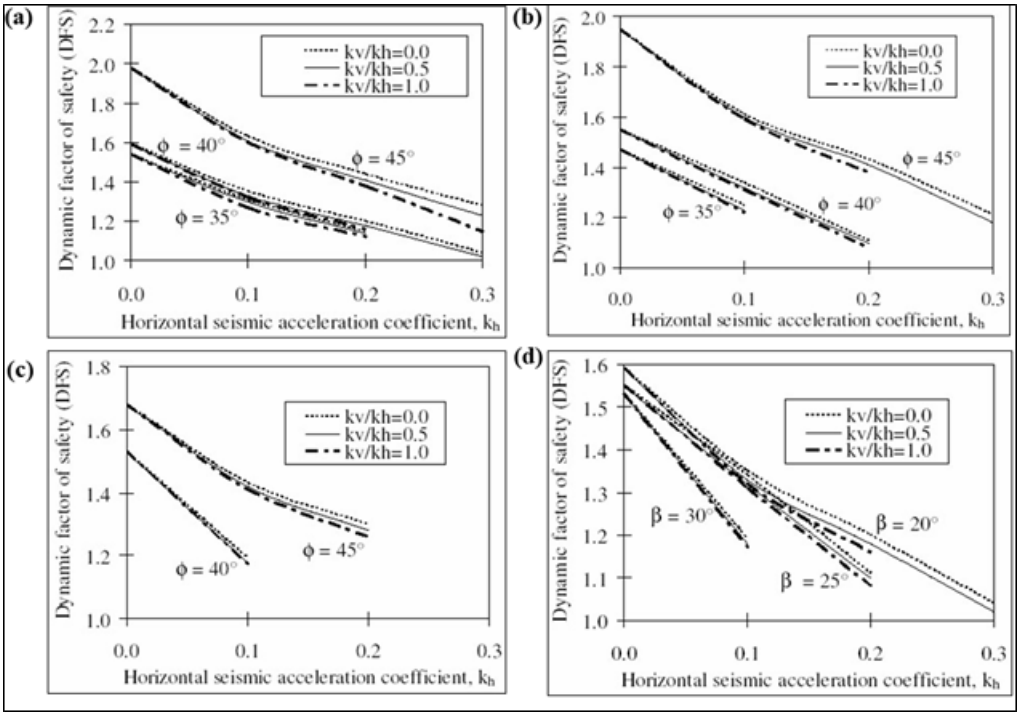

Figure 2: *(a) Variation of DFS with* k_h *for* $\beta = 20°$*, (b) Variation of DFS with* k_h *for* $\beta = 25°$*, (c) Variation of DFS with* k_h *for* $\beta = 30°$*, (d) Variation of DFS with* k_h *for* $\phi = 40°$ *[27].*

3.2 The Effect of Change k_h and k_v: FEM Method

Zhou and Qin [15] developed a finite-element upper-bound framework that incorporated pseudo-dynamic acceleration functions to analyze seismic slope stability. Their results clearly demonstrate that as k_h increased from 0.1 to 0.3 , the safety factor decreased nonlinearly, especially under pseudo-dynamic conditions. In contrast to LEM, which assumes instantaneous uniform loading, their FEM model considered time-varying wave propagation and soil deformation. Notably, the inclusion of k_v had a significant compounding effect, further reducing the slope's stability by modifying stress distributions across the failure plane. This analysis confirmed that FEM is more sensitive and realistic in evaluating the impact of seismic parameters on slope behavior.

Figure 3 illustrates the strong inverse relationship between k_h and the FQS for slopes with varying friction angles, as analyzed using a finite-element upper-bound method with a pseudo-dynamic approach. As k_h increases, the FoS declines noticeably, with this reduction being more severe at lower ϕ values. Slopes with higher friction angles (e.g., $\phi = 40°$) retain greater stability under seismic loading, while those with lower φ (e.g., $\phi = 25°$ or $30°$) become critically unstable even at moderate seismic coefficients ($k_h \geq 0.2$). This trend highlights that both material strength and seismic intensity are key factors in determining slope performance.

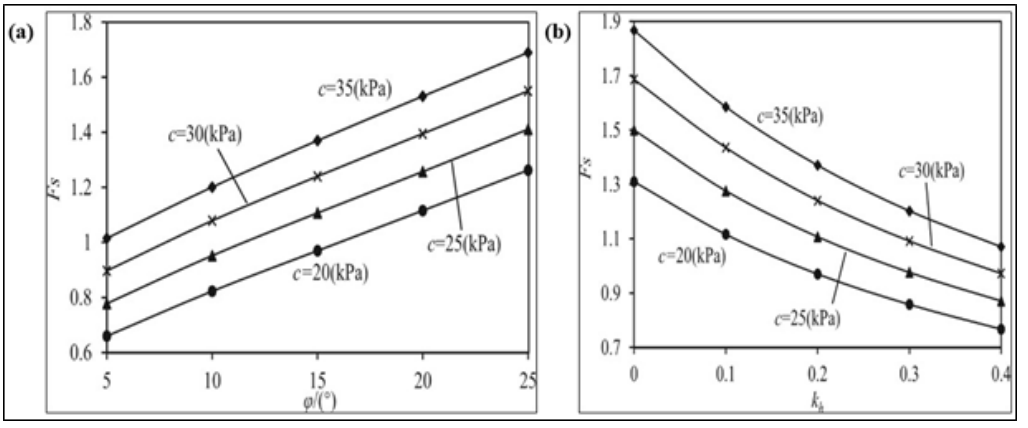

Figure 3: *(a) Influence of soil shear strength on the factor of safety, (b) Influence of seismic coefficient* (k_h) *on the factor of safety [20].*

4. Comparison of the Effect of Different Soil Models on FoS

In finite element-based slope stability analysis, the choice of soil constitutive model is a key factor determining the accuracy of the FoS and the predicted failure mechanism. Different soil models reproduce the stress-strain behavior of geomaterials in distinct ways, particularly under seismic or high-stress loading conditions. Güllü [28] compared three commonly used soil models-MohrCoulomb, Hardening Soil, and Linear Elastic-within a two-dimensional FEM framework under various loading scenarios. The study concluded that the Mohr-Coulomb and Hardening Soil models yielded similar and reliable FoS values, whereas the Linear Elastic model significantly overestimated slope stability, failing to capture plastic deformation and stress redistribution under load. Liu et al. [29] further examined the influence of the Drucker-Prager (D-P) and MohrCoulomb (M-C) models in FEM-based slope analysis. Although both models produced comparable FoS results when appropriately calibrated, the D-P model exhibited greater adaptability under complex plasticity conditions. Liu et al. also reported that plastic parametersnotably cohesion and internal friction angle-exert the most significant influence on FoS, while elastic parameters, such as Poisson's ratio, play a secondary role. Similarly, Tan and Wang [30] conducted a nonlinear FEM study incorporating large-deformation and elastoplastic behavior. Their results confirmed that three-dimensional large-deformation models based on the MohrCoulomb criterion produce higher and more realistic FoS values compared to simplified twodimensional small-deformation analyses. These findings reinforce that a realistic representation of stress-strain behavior-particularly through elastoplastic and strain-dependent stiffness modelsleads to more accurate and physically meaningful slope stability predictions (Table 4).

Table 4: *Comparison of the effect of different soil models on FoS [35–38].*

Soil Model	Behavior Under Seismic Loading	Effect on (FoS)
Linear Elastic (LE)	Only elastic deformation; ignores plasticity and softening.	Overestimates FoS; unsafe for seismic slope analysis.
Mohr-Coulomb (MC)	Elastic-perfectly plastic; no strain softening or cyclic degradation.	Moderate FoS; may overpredict stability under earthquake loading.
Hardening Soil (HS)	Nonlinear hardening, stress-dependent stiffness; accounts for plastic strain.	Lower and more realistic FoS under seismic conditions.
Hardening Small-Strain (HSS)	Includes small-strain stiffness (Gmax degradation) and hardening effects.	Most conservative and reliable FoS for cyclic seismic loading.
Softening / Kinematic Hardening	Cyclic stiffness degradation, post-peak softening, strain weakening.	Lowest but most realistic FoS; captures post-yield strength reduction.

5. Duration of Earthquake Effect on FoS

Another important factor to be considered when conducting a slope stability analysis is the duration of an earthquake, as it significantly impacts the factor of safety of slopes. A longer peak response period (a longer earthquake duration) leads to a decreased factor of safety. This is due to the slope experiencing strong shaking for a longer period of time, allowing more deformation and progressive failure to develop. An artificial amplitude of seismic acceleration with various peak response periods was studied using the Explicit Finite Element Method (EFEM) to reach this conclusion [35]. Moreover, Yanhong et al. [36] also reported that the factor of safety is directly affected by the duration of the earthquake and the variation of seismic loads. They noted that prolonged loading induces progressive plastic deformation. This leads to a time variation of the factor of safety, where there is a high risk of failure after about 30 seconds of seismic loading. Their genetic algorithm (GA) and dynamic finite element analysis (DFEA) also identified that prolonged durations of earthquakes produce continuous weakening of slope strength due to the buildup of stress.

6. Effect of Simulating Earthquake Dynamic Loading on FoS

It is important to account for the soil's dynamic mechanical behavior and simulate the dynamic loading from an earthquake to calculate the FoS for seismic slope stability appropriately. Simulating an earthquake is, however, a broad area of study, since differing types of dynamic loading result in differing factors of safety. The types of dynamic loading can differ among pseudostatic analysis, cyclic loading, or laboratory-like loading. A time- and space-varying seismic acceleration was applied by Zhou and Qin [15], employing a coupled finite-element upper-bound analysis and pseudo-dynamic approach to study seismic slope stability. Their approach applied input time- and space-varying seismic acceleration and demonstrated that pseudo-dynamic solutions are more prone to producing higher FoS values than the overly conservative pseudostatic methods.

The study highlighted FoS sensitivity to the soil strength parameters and to seismic wave characteristics such as phase difference and period. In turn, Ma et al. [35] used an EFEM that involved a dynamic visco-elasto-plastic constitutive model to investigate processes and stability of slope failure due to earthquakes. Their evidence showed that unless the soil dynamic behavior (e.g., damping and degradation of the shearing modulus) is considered, FoS values are unrealistic, and soil dynamics are required for realistic seismic loading. Conventional pseudo-static approaches were also found to result in an underestimation of slope stability by both studies, but Ma et al. [35] also showed that characteristics of ground motion, including the rate of acceleration and the response period, affect FoS significantly; higher acceleration and longer periods are equivalent to reduced stability. While Zhou and Qin [15] concentrated on the optimization of upper-bound solutions using application of

linear programming, Ma et al. [35] shed light on sliding distances and progressive failure processes and showed that post-failure behavior is largely controlled by frictional resistance.

7. Model Validation

In the study of dynamic slope stability, an essential initial step is to validate the numerical model to ensure the reliability and accuracy of the simulation outcomes. However, validation using FEM poses significant challenges. A major difficulty arises from the scarcity of comprehensive studies that provide full documentation of simulation data. Many existing research works omit critical details, such as the specific characteristics of earthquake loading input, mesh configurations, boundary conditions, geometry dimensions, and damping parameters. Furthermore, inconsistencies among different studies are exacerbated by the use of various software platforms and modeling approaches, thereby complicating direct comparisons and replication efforts. Given these limitations, the present work adopts a validation approach based on the study conducted by Jacob and Venkataramana [37], which applied the pseudo-static method using PLAXIS software. This reference was selected because it aligns closely with the intended simulation conditions and provides sufficient data to facilitate meaningful comparisons.

The material properties incorporated into the model are consistent with those used in the validation reference. The soil is modeled as a Mohr-Coulomb material under drained conditions. Table 5 summarizes the detailed soil properties applied in the analysis. The slope geometry, shown in Figure 4, consists of a 3-meter-high slope atop a 6-meter-high base, with the slope inclined at a ratio of 1H : 1 V. The total model length extends 22 meters, segmented into a 9 -meter horizontal section, a 3 -meter sloped section, and a 10 -meter horizontal section. An earthquake acceleration of 0.2 g was employed to simulate dynamic loading conditions. Boundary conditions were carefully assigned, with the lateral sides fixed in the horizontal direction and the bottom boundary fixed in both directions. A zero-degree dilatancy angle and a Poisson's ratio of 0.3 were assigned, with a modulus of elasticity of $30,000 \text{kN/m}^2$.

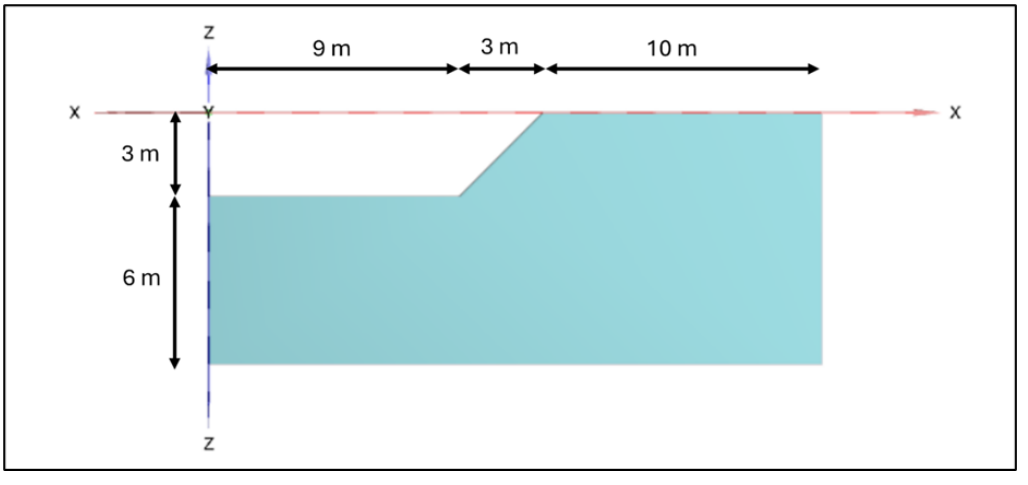

Figure 4: *Slope geometry and domain configuration used in FEM validation model.*

The mesh was generated with medium density refinement to balance computational efficiency and accuracy. Damping was considered in accordance with Rayleigh damping specifications, though specific coefficients were adopted from standard recommendations due to the lack of explicit data in prior studies.

The factor of safety resulting from this FEM analysis using PLAXIS 3D was 3.47, which is

Table 5: *Soil properties input used for model validation [44].*

Parameters Considered	Values	Units
Material model	Mohr–Coulomb	–
Internal friction angle	40	Degree (°)
Cohesion	25	kN/m^2
Total unit weight ()	18.5	kN/m^3
Saturated unit weight (sat)	20	kN/m^3
Modulus of elasticity	30,000	kN/m^2
Poisson's ratio	0.3	–
Dilatancy angle	0	Degree (°)

remarkably close to the value of 3.40 reported by Jacob and Venkataramana [37]. This close agreement supports the validity of the numerical model developed for this study. Additionally, to further corroborate the results, an LEM analysis was conducted using Slide2 software, employing both Bishop's and Spencer's methods. The FoS values obtained were 3.36 and 3.41, respectively, again demonstrating a close correlation with the FEM results (Table 6).

Table 6: *Comparison of (FoS) values.*

Reference	Method	FoS
Jacob and Venkataramana [44]	FEM (PLAXIS 2D)	3.40
Current Study	FEM (PLAXIS 3D)	3.47
Current Study	LEM (Slide2 - Bishop Method)	3.36

As demonstrated, the results obtained from both the FEM and LEM approaches are closely aligned with the reference study, thereby validating the modeling approach adopted herein for the investigation of dynamic slope stability under pseudo-static conditions.

8. Simulation Setup

8.1 Material Properties

The material properties assigned in the model were chosen to closely represent real field conditions. These properties were sourced from a well-established reference database provided by Brinkgreve et al. [38], ensuring that the modeled soil parameters are realistic and grounded in experimental data. Table 7 summarizes the soil parameters used for the simulations.

The geometry of the numerical model was carefully designed to meet criteria recommended by prior studies for dynamic analysis. As shown in Figure 5, the lateral extent of the model was selected as 20 meters, which exceeds four times the slope height (4H), ensuring the minimization of wave reflection effects at the model boundaries. This approach is consistent with the recommendations by Van Der Kwaak [39], who emphasized the importance of extending domain boundaries to mitigate spurious wave reflections during dynamic loading. Similarly, the vertical domain depth was set at 16 meters, equivalent to four times the slope height (4H), thus satisfying the recommendation that the depth should be at least two times the slope height (2H) as suggested by Zewdu [40]. This rigorous attention to model dimensioning enhances the accuracy of the dynamic response simulation and reduces boundary condition artifacts, providing a solid foundation for reliable interpretation of the results.

*Shear modulus at very small strains, **Reference shear strain at 70% of G_0, ***Stress dependent stiffness according to a power law

Table 7: *Soil properties used in the dynamic simulation.*

Parameters Considered	Value	Units
Total unit weight (γ)	17	kN/m^3
Saturated unit weight (γ_{sat})	19.8	kN/m^3
Secant stiffness ($E_{50}{}^{ref}$)	30,000	kN/m^2
Tangent stiffness ($E_{oed\ ref}$)	30,000	kN/m^2
Elastic unloading / reloading (E_{ur}^{ref})	90,000	kN/m^2
Poisson's ratio (v)	0.2	–
Shear Modulus $(G_0^{ref})^*$	94,000	kN/m^2
Shear Strain $(\gamma_{0.7})^{**}$	0.00015	–
Internal friction angle (φ)	34.3	Degree (°)
Cohesion (c)	0	kN/m^2
Dilatancy angle (ψ)	4.3	Degree (°)
Stress power (m)***	0.544	–

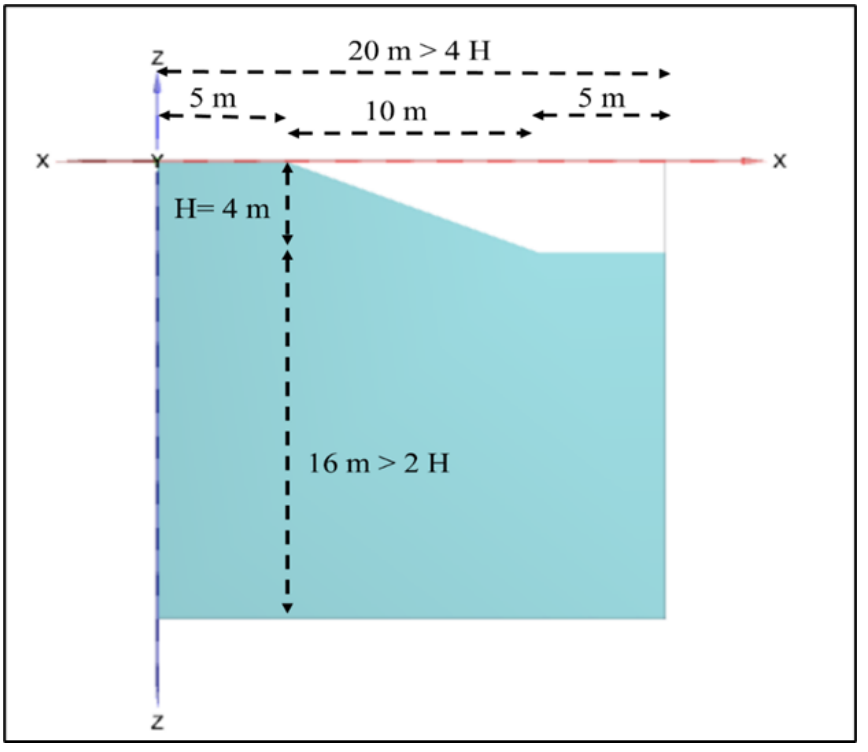

Figure 5: *Model geometry and boundary extents for dynamic analysis based on recommended domain criteria.*

In this study, the Mohr–Coulomb constitutive model was adopted specifically for the pseudo-static analysis, in order to enable a fair comparison between the FEM results and those obtained from the LEM. The Mohr–Coulomb model is widely used in such contexts due to its simplicity and its ability to capture fundamental strength parameters under seismic conditions, making it suitable for benchmarking against previous research. However, for more advanced simulations involving the input of actual recorded earthquake time histories and harmonic cyclic loading, the Hardening

Soil model with small-strain stiffness (HS Small) was implemented. The HS Small model accounts for nonlinear stiffness degradation and strain-dependent shear modulus variation, thereby offering enhanced accuracy in capturing the dynamic response of soils subjected to strong ground motions.

8.2 Dynamic Boundary Condition

In dynamic analysis, accurately representing boundary conditions is critical because, in reality, seismic waves propagate infinitely through the soil medium. In contrast, in numerical simulations with conventional fixed boundaries, seismic waves are reflected back into the model, leading to unrealistic amplification and interference effects that can distort the results. Therefore, it is essential to implement boundary conditions that can absorb outgoing waves and simulate free-field conditions.

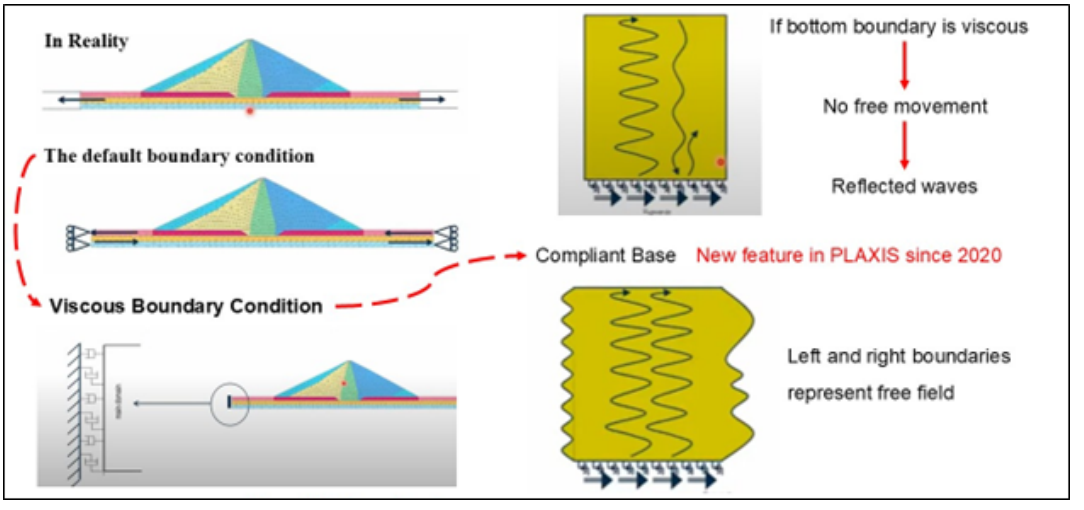

Figure 6: *Illustration of boundary condition types in PLAXIS dynamic analysis, including default fixed boundaries, viscous boundaries, and compliant-base boundaries, and their effects on wave reflection and free-field behavior.*

To address this, the current study adopted a viscous boundary approach as a simplified yet effective method for minimizing wave reflections. In this method, dashpots are introduced at model boundaries, functioning as mechanical devices that resist motion proportionally to velocity, similar to shock absorbers. These viscous boundaries absorb outgoing seismic energy and prevent its reflection into the model domain. However, this approach comes with certain limitations: viscous boundaries are most effective for normally incident waves and lose accuracy when waves are inclined relative to the boundaries. Moreover, to maintain acceptable accuracy, boundaries must be placed sufficiently far from critical areas of interest, ensuring that any minor reflections do not affect key results.

The lateral boundaries were treated using free-field conditions, representing the motion of semi-infinite soil domains during an earthquake. The bottom boundary was modeled as a viscous boundary with dashpots to simulate energy dissipation, in accordance with standard practices for seismic site response analysis. However, a notable limitation of using prescribed displacement or acceleration at the bottom boundary is the assumption of a rigid base, which restricts the natural free movement of dashpots and may lead to partial reflection of seismic waves, especially at high frequencies. To overcome this, more advanced boundary conditions — such as compliant base boundaries — have been developed and were incorporated into PLAXIS software updates in 2020. These compliant bases enable accurate simulation of incoming seismic waves by allowing vertical-only motion without rigid constraints, thus eliminating spurious reflections. A conceptual illustration of the differences

between real boundary behavior, default fixed boundaries, viscous boundaries, and compliant-base boundaries in PLAXIS is presented in Figure 6.

The boundary condition setup used in this study was determined by carefully reviewing and following best practices described in the literature. Lateral domain extents and vertical domain depths were chosen based on recommendations to ensure sufficient distances for minimizing artificial reflections, while the viscous boundary method was selected as a practical and validated approach for simulating dynamic earthquake loading in finite models. This combination of viscous side boundaries, a viscous bottom boundary, and large model dimensions provides an effective balance between computational efficiency and physical realism, ensuring the reliability of the dynamic slope stability results obtained.

8.3 Earthquake Input Data

To simulate the dynamic response of the slope under realistic seismic loading, recorded earthquake ground motions were obtained (https://www.strongmotioncenter.org) from the Strong Motion Virtual Data Center (VDC). Two different earthquake records were selected, covering a range of magnitudes, peak ground accelerations, and source distances. Table 8 presents the details of the selected events, including the earthquake name, location, year, and maximum recorded acceleration (a_{max}). The time histories of acceleration for the selected earthquake records are illustrated in Figure 7. These acceleration-time plots highlight the variation in amplitude, frequency content, and duration among the different seismic events, providing a diverse set of loading scenarios to evaluate the dynamic stability of the slope model (Table 8).

Table 8: *Summary of selected earthquake records.*

Earthquake Name	EQ Location	EQ Year	Max. Acceleration (g)
Arthurs Pass Police Station	New Zealand	1992	0.24
Chiayi Earthquake	Taiwan	1999	0.28

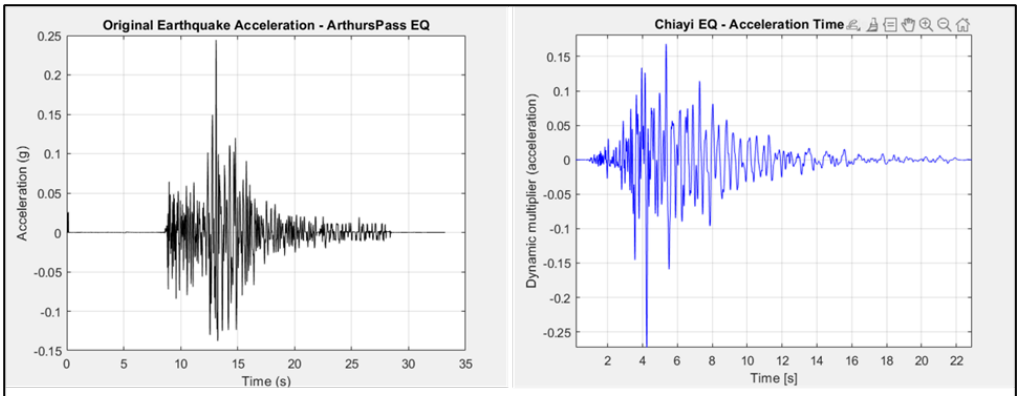

Figure 7: *Time histories of original earthquake accelerations used for dynamic input.*

Although these records were obtained from different seismic stations located at varying distances from their respective epicenters, in this study, each acceleration record was applied directly as input motion without further modification. This approach inherently considers the local site effects already embedded in the original recordings, which include amplification, damping, and filtering effects

of the local soil conditions at the recording stations. As such, the dynamic analyses realistically incorporate these site effects without the need for separate site response corrections.

In dynamic numerical modeling, several approaches are available to apply earthquake-induced loading to the slope model. In this study, three different methods were employed to introduce dynamic effects into the simulations using PLAXIS 3D software, each offering distinct advantages depending on the objective of the analysis.

The first method involves performing pseudo-static analysis, in which the seismic effect is approximated by applying a constant horizontal acceleration throughout the model. k_h is assigned based on the amax associated with the considered earthquake. Following common practice, the seismic coefficient is determined as two-thirds of the peak ground acceleration, as shown in Equation (5). This empirical relationship has been widely adopted in the literature [41,42], providing a conservative estimation of earthquake effects for stability assessment.

$$k_h = (2/3)a_{\max} \tag{5}$$

In this study, a range of vertical-to-horizontal seismic coefficient ratios (k_v/k_h) was analyzed to reflect the diversity of design assumptions and regional seismic considerations found in practice. k_v, while typically less dominant than k_h, can significantly affect the FoS, particularly under strong vertical ground motions or near-fault conditions. The inclusion of various (k_v/k_h) ratios enables the evaluation of slope response under both simplified and conservative seismic loading assumptions.

Neglecting vertical acceleration altogether ($k_v = 0$) represents one of the earliest and most commonly used simplifications in U.S. practice, based on the premise that vertical accelerations are short in duration and often out-of-phase with slope deformation [43]. However, this approach may underpredict potential failure in regions experiencing strong vertical ground shaking. A more balanced and widely accepted method assumes ($k_v = 0.5k_h$), consistent with empirical ground motion observations and supported by Kramer [42], IS 1893:2016, and Eurocode 8 (EN 1998-5), making it a standard design value in many international codes. To capture more conservative scenarios-especially applicable in near-fault zones or when vertical acceleration is amplified due to site effects-the case of ($k_v = k_h$) is also evaluated. This assumption has been used by Makdisi and Seed [44] and incorporated into pseudo-dynamic analyses by Choudhury and Nimbalkar [45], who showed that vertical components may considerably increase the likelihood of failure when synchronized with horizontal motion.

By systematically varying (k_v/k_h) from 0 to 1.0, this study quantifies how increasing vertical inertial forces affect slope stability under different seismic intensities. The results provide insight into the range of safety margins predicted under each assumption, demonstrating that vertical acceleration, though often simplified, should not be ignored in critical or high-risk seismic designs.

The second method directly applies the original recorded earthquake acceleration time histories obtained from the VDC, as presented previously in Figure 7. In this approach, the accelerationtime series are imposed at the model base, allowing for a realistic simulation of the dynamic response by capturing the true variability of seismic loading in time and intensity.

The third method introduces cyclic dynamic loading, replicating conditions similar to cyclic shear tests conducted at the laboratory scale. In this approach, the recorded earthquake signals are approximated by a harmonic function defined by amplitude (A), frequency (f), and phase ($\emptyset$). The applied acceleration (a) function is expressed mathematically in Equation (6).

$$a(t) = A * \sin(2\pi ft + \emptyset) \tag{6}$$

t is time in seconds. This formulation allows for simplified yet controlled cyclic loading simulations, closely aligning with cyclic soil behavior studies under laboratory conditions. This method was implemented based on the procedures outlined by Kramer [51] in "Geotechnical Earthquake

Engineering" (Chapter 7) and further supported by the PLAXIS Dynamics Manual (Harmonic Load section).

To achieve harmonic representation from the real earthquake records, MATLAB was utilized to extract the dominant frequency content and amplitude characteristics from the acceleration time histories. This approach provides an additional perspective on soil behavior under idealized cyclic loading and facilitates comparisons between actual and simplified dynamic load cases. The comparison between the original recorded earthquake accelerations and their corresponding harmonic approximations is presented in Figure 8. As shown, while the harmonic signals capture the main frequency characteristics of the seismic records, they present an idealized and regular cyclic pattern compared to the irregular, complex nature of the real earthquake motions.

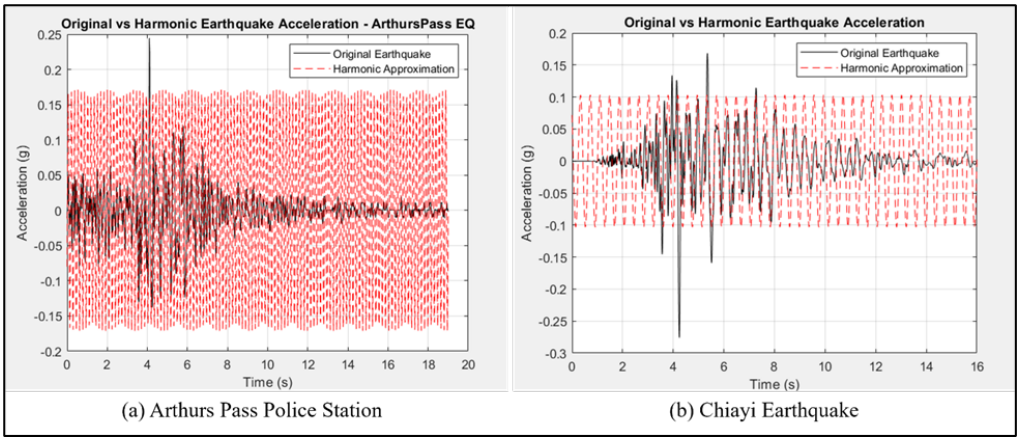

Figure 8: *Original and harmonic earthquake acceleration records.*

9. Results and Discussions

9.1 Effect of Horizontal and Vertical Seismic Coefficients on Slope Stability: Comparative Analysis Between LEM and FEM in Pseudo-Static Framework

A series of pseudo-static analyses was conducted to examine the influence of horizontal and vertical seismic coefficients on the FoS of dry slopes. The vertical seismic coefficient was expressed as a ratio of the horizontal component (k_v/k_h), reflecting a range of estimation approaches used in practice. For each combination, FoS values were computed using both the LEM via Slide2 and the FEM via PLAXIS 3D, employing the Mohr-Coulomb failure criterion. The corresponding results are summarized in Table 9 and illustrated in Figure 9.

The results presented in Figure 9 and the accompanying table clearly indicate a systematic reduction in FoS with increasing k_h, consistent across both LEM and FEM analyses. At $k_h = 0$, the FoS values of 1.706 (LEM) and 2.018 (FEM) indicate stable slope conditions under static loading. However, as k_h increases to 0.20 , the FOS values drop significantly to 0.945 (LEM) and 1.123 (FEM), signifying a transition toward marginal or unstable behavior under higher inertial forces. This trend is in agreement with the findings of Yang et al [46], who reported that increases in pseudo-static accelerations substantially reduce FoS, with slopes becoming critically unstable beyond specific threshold levels.

The influence of k_v is also evident in the results. For each fixed k_h, increasing k_v generally leads to a measurable reduction in FoS, with the effect becoming more significant when k_v approaches or exceeds approximately $0.75k_h$. This observation aligns with the work of Choudhury and Nimbalkar [45], who highlighted that vertical seismic loading-particularly at higher proportions of k_h-can

intensify internal stress demands and aggravate failure mechanisms within slopes. Kramer [42] similarly emphasized the importance of vertical ground motions, especially in nearfault conditions, and their relevance in pseudo-static slope stability evaluations. While some design practices simplify seismic analyses by assuming $k_v = 0$ [43], other standards, such as the Indian seismic code IS 1893:2016, recommend using $k_v = 0.5k_h$, a value that corresponds reasonably well with recorded ground-motion ratios.

Table 9: *Variation of (FoS) with different horizontal and vertical seismic coefficients using LEM and FEM.*

k_h	k_v/k_h	k_v	FoS (LEM - Slide 2)	FoS (FEM -Plaxis)
0.00	0.00	0.00	1.706	2.018
0.05	0.00	0.00	1.486	1.749
	0.25	0.01	1.484	1.746
	0.50	0.03	1.48	1.741
	0.75	0.04	1.478	1.739
	1.00	0.05	1.476	1.734
0.10	0.00	0.00	1.31	1.559
	0.25	0.03	1.301	1.545
	0.50	0.05	1.294	1.54
	0.75	0.08	1.283	1.515
	1.00	0.10	1.276	1.517
0.15	0.00	0.00	1.166	1.388
	0.25	0.04	1.15	1.362
	0.50	0.08	1.133	1.341
	0.75	0.11	1.119	1.322
	1.00	0.15	1.1	1.304
0.20	0.00	0.00	1.046	1.241
	0.25	0.05	1.022	1.207
	0.50	0.10	0.999	1.172
	0.75	0.15	0.974	1.15
	1.00	0.20	0.945	1.123

A comparative assessment of the two analytical approaches shows that FEM consistently yields higher FoS values than LEM for all combinations of k_h and k_v [47,48]. For instance, at $k_h = 0.10$ and $k_v = 0.05$, the FoS values are 1.294 (LEM) and 1.540 (FEM), reflecting an approximate 19% increase in the FEM prediction. Across all cases in this study, FEM results are about 17 – 19% higher than those obtained using LEM, which is consistent with the findings of Siregar et al. [49], who reported that FEM-based FoS estimates are generally 9 – 10% higher due to the method's ability to capture stress redistribution, progressive yielding, and deformation compatibilitymechanisms that are inherently idealized or simplified in traditional LEM frameworks.

9.2 Effect of Soil Model Type and Mesh Size on Pseudo-Static Slope Stability Using Recorded Earthquake Data

To evaluate the sensitivity of slope stability to modeling assumptions and earthquake ground motion intensity, two recorded seismic acceleration histories, Arthurs Pass Police Station ($a_{max} = 0.24$ g) and Chiayi Earthquake ($a_{max} = 0.28$ g), were selected for analysis. The a_{max} for each earthquake was converted into k_h using the widely adopted empirical relationship $k_h = (2/3)a_{max}$ [42] and adopted by several researchers (e.g., Choudhury and Nimbalkar [45]). The resulting k_h values were

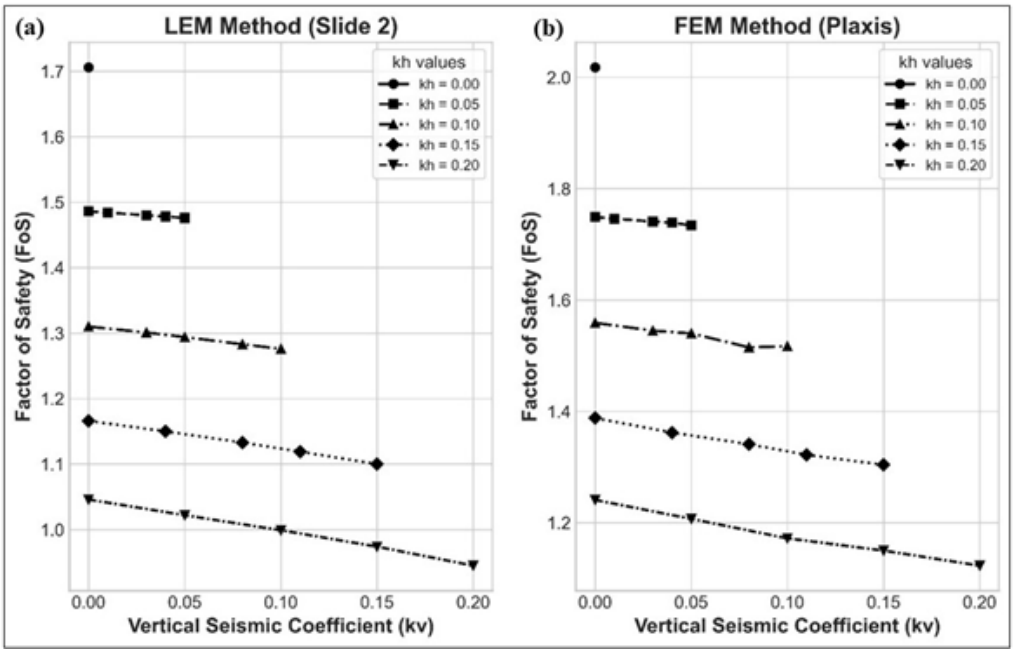

Figure 9: *Factor of safety trends for varying vertical seismic coefficients (* k_v *) under different horizontal seismic coefficients (kb), computed using: (a) LEM, (b) FEM.*

0.16 and 0.18 , respectively (Table 10).

To assess the influence of vertical seismic loading, a series of vertical-to-horizontal seismic coefficient ratios (k_v/k_h) ranging from 0 to 1 were applied, corresponding to practical estimation scenarios discussed by Seed and Whitman [43], IS 1893:2016, and Eurocode 8. Each case was analyzed using the LEM with the Mohr-Coulomb model, and the FEM in PLAXIS under four configurations:

- Mohr–Coulomb (Medium Mesh)
- Mohr-Coulomb (Fine Mesh)
- Hardening Soil with Small-Strain Stiffness (HS small, Medium Mesh)
- HS small (Fine Mesh)

Table 10 and Figure 10 collectively demonstrate a clear and systematic reduction in the FoS with increasing k_b and k_{ag} for both earthquake records. In the LEM analyses illustrated in subplots (a) and (c), the FoS exhibits an almost linear decline as k_c increases, reflecting the direct and cumulative influence of seismic inertia forces on the reduction of shear resistance. This behavior is characteristic of LEM formulations, which apply seismic coefficients uniformly across the sliding mass without accounting for internal stress redistribution. As a result, the LEM predictions inherently portray a progressive and proportional loss of stability under combined seismic loading. In contrast, the FEM results displayed in subplots (b) and (d) consistently yield higher FoS values relative to the LEM predictions for all combinations of k_h and k_b. This is attributed to the FEM's ability to capture stress redistribution, non-linear stiffness degradation, and deformation compatibility within the soil mass-mechanisms that are absent in LEM approaches. Consequently, FEM modelling provides a more realistic representation of slope behavior under seismic loading, often moderating the destabilizing effect suggested by LEM.

A comparison of the Mohr-Coulomb and HS Small constitutive models indicates that both models

Table 10: *Comparative factor of safety analysis under pseudo-static loading using LEM and FEM with varying seismic coefficients, soil models, and mesh sizes.*

EQ Name	Max $a_{max.}$	$k_k(g)$	$\mathbf{k}_s/\mathbf{k}_h$	k_k	FoS (LEM-Slide2)	FoS (FEM – PLAXIS)			
						Mohr Coulomb (Medium Mesh)	Mohr Coulomb (Fine Mesh)	HS Small (Medium Mesh)	HS Small (Fine Mesh)
Arthurs Pass Police Station	0.24	0.16	0.00	0.00	1.14	1.355	1.272	1.349	1.265
			0.25	0.04	1.124	1.337	1.259	1.33	1.247
			0.50	0.08	1.106	1.302	1.227	1.309	1.221
			0.75	0.12	1.087	1.287	1.209	1.287	1.2
			1.00	0.16	1.067	1.263	1.182	1.261	1.178
Chiayi Earthquake	0.28	0.18	0.00	0.00	1.092	1.298	1.217	1.292	1.206
			0.25	0.05	1.07	1.256	1.187	1.268	1.178
			0.50	0.09	1.051	1.247	1.163	1.246	1.157
			0.75	0.14	1.025	1.217	1.147	1.214	1.133
			1.00	0.18	1.003	1.187	1.122	1.189	1.108

produce closely aligned FoS estimates, with discrepancies typically falling within $1 - 3\%$ across the full range of seismic coefficients and mesh densities. For example, in the Chiayi Earthquake scenario at $k_{ct} = 0$, the fine-mesh FEM analyses yield FoS values of 1.217 for the Mohr-Coulomb model and 1.206 for the HS Small model. Even at the highest seismic demand considered ($k_{kc} = 0.18$), the fine-mesh FoS values remain closely matched at 1.122 and 1.108, respectively. These modest differences suggest that while both constitutive models provide equivalent shear strength representation, the HS Small model-owing to its enhanced stiffness formulation and consideration of strain-dependent small-strain shear modulus-tends to produce slightly more conservative FoS estimates under elevated seismic loading.

This observation is consistent with guidance from the PLAXIS Material Models Manual [50], as vell as findings reported by Das et al. [51], who emphasize that deviations between these models arise primarily from stiffness-related behavior rather than differences in ultimate shear strength.

Mesh density was also found to exert a systematic influence on computed FoS values. Across both constitutive models and earthquake scenarios, fine meshes consistently produced lower FoS values han medium meshes, typically by $2 - 7\%$. For instance, in the Chiayi Earthquake case at $k_v = 0.09$, he HS Small model yields FoS values of 1.246 for the medium mesh and 1.157 for the fine mesh, eflecting a substantial reduction attributable to improved numerical resolution. Finer meshes allow more accurate modelling of stress concentrations and better capture the localization of shear trains, thus producing more realistic and conservative stability estimates. This behavior is well locumented in numerical modelling literature; Mohd and Kasa [52] and Lin et al. [53] both eported that coarse meshes tend to diffuse the failure mechanism and artificially distribute strain, which can result in overly optimistic FoS predictions due to inhibited shear band formation.

Taken together, the comparative results across analysis methods, constitutive models, and mesh densities provide a coherent and technically robust understanding of the seismic stability behavior of the slope. The collective evidence reinforces established theoretical and empirical findings, showing that increasing seismic demand leads to a systematic reduction in stability, while the FEM frame-

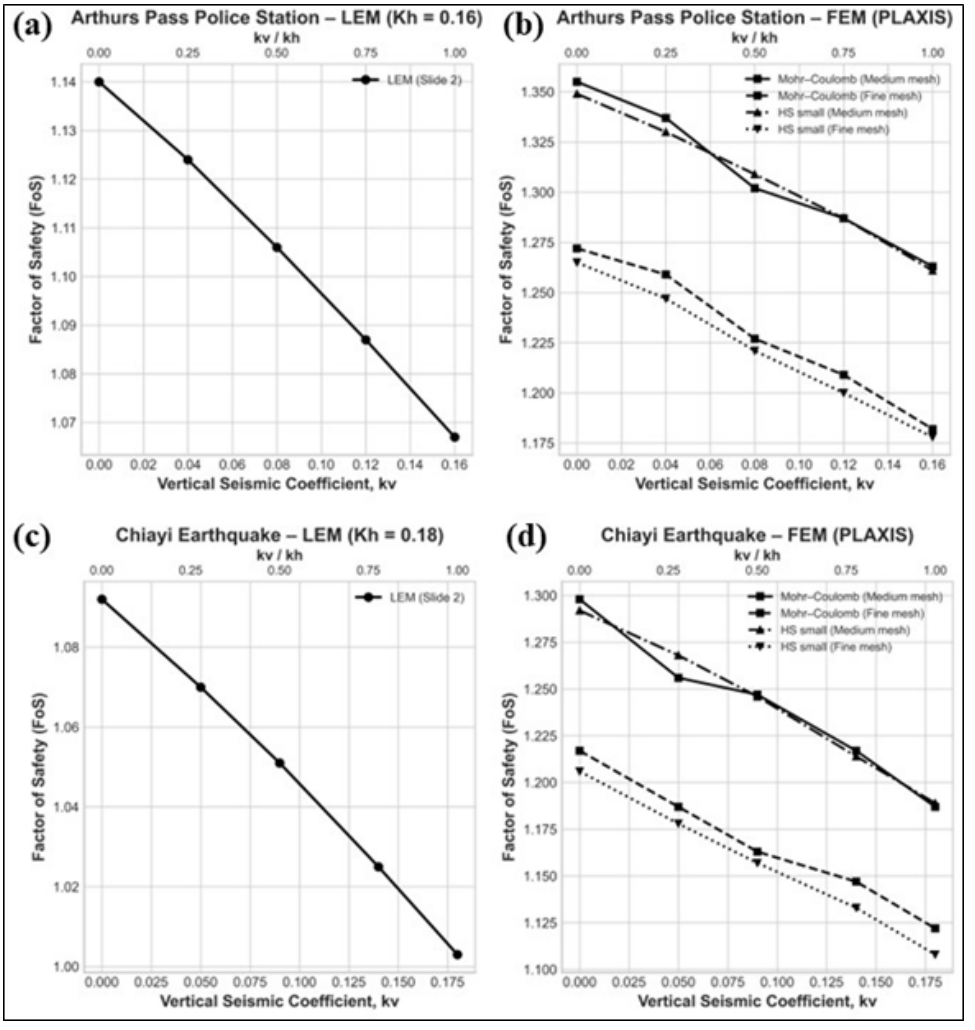

Figure 10: *FoS results for (a) Arthurs Pass–LEM, (b) Arthurs Pass–FEM, (c) Chiayi–LEM, and (d) Chiayi–FEM. FoS decreases with increasing* k_v*, with FEM giving slightly higher values and only minor differences between constitutive models and mesh densities.*

work—by capturing stress redistribution and deformation compatibility—produces more realistic and generally higher FoS estimates than those obtained from LEM. The close alignment between the Mohr–Coulomb and HS Small models further demonstrates the consistency of the FEM predictions, with the slightly lower FoS values from HS Small reflecting the influence of its enhanced stiffness formulation and small-strain behavior on the mobilized shear response. Moreover, the sensitivity of the results to mesh refinement highlights the importance of numerical resolution in accurately representing shear localization and internal stress paths, with fine meshes consistently yielding more conservative and reliable assessments of seismic performance. Collectively, these interrelated observations confirm the validity of the modelling approach and underscore the critical parameters governing seismic slope stability in numerical analyses.

9.3 Comparison of Earthquake Loading Methods in FEM Analysis

To investigate the influence of different earthquake loading strategies on slope stability, a comparative analysis was conducted using the FEM for two earthquake records: the Arthurs Pass (New Zealand, 1992) and Chiayi (Taiwan, 1999) events. Each case was analyzed using three seismic input methods: (1) pseudo-static loading based on a seismic coefficient $k_h = (2/3)a_{max}$ and $k_v = 0.5k_h$, (2) actual dynamic acceleration time histories, and (3) idealized cyclic harmonic loading calibrated to the same peak amplitude and duration.

In the pseudo-static analyses, the computed FoS were 1.221 and 1.157 for the Arthurs Pass and Chiayi earthquakes, respectively. These values served as the baseline for comparison. When the actual recorded accelerations were used in dynamic time-history FEM simulations, the resulting FoS increased modestly to 1.295 and 1.226 , respectively. This is consistent with the findings of Sazzad and Biman [54] and Eikebrokk and Kaynia [55], who observed that full dynamic analyses often yield $5 - 8\%$ higher FoS than pseudo-static methods due to transient shaking effects, stress redistribution, and the damping behavior of soils during seismic loading.

Table 11: *Comparison of (FoS) for different earthquake loading methods using FEM for Arthurs Pass and Chiayi earthquakes*

EQ Name	FoS (Pseudo- Static)	FoS (Actual EQ loading)	FoS (Cyclic Loading)
Arthurs Pass Police Station	1.221	1.295	1.099
Chiayi Earthquake	1.157	1.226	1.041

Conversely, when harmonic loading was applied-designed to replicate the dominant frequency and amplitude of the real earthquake-the FoS decreased to 1.099 (Arthurs Pass) and 1.041 (Chiayi). These values reflect a $\sim 10\%$ reduction from pseudo-static outcomes and align with the work of Ismail et al. [56], who demonstrated that simplified cyclic inputs can induce more severe failure mechanisms, especially when their frequency content resonates with the natural frequency of the slope. Table 11 presents a comparison of the computed FoS obtained from the pseudo-static, actual earthquake loading, and cyclic loading methods using FEM for the Arthurs Pass and Chiayi earthquakes.

10. Limitations and Future Research Directions

Although this study provides valuable insights into the comparative performance of the LEM and FEM for seismic slope stability analysis, certain limitations should be acknowledged. Recognizing these limitations not only helps define the scope of the findings but also highlights opportunities for further research to enhance the reliability and practical applicability of seismic slope modeling.

10.1 Limitations

• The study considered a single, idealized slope geometry with homogeneous soil, which does not capture the complexity of natural slopes with layered stratigraphy, variable geometry, or rock–soil interfaces.

• Only dry and fully drained conditions were analyzed, meaning pore pressure generation, cyclic softening, and liquefaction effects were not incorporated, limiting applicability to saturated or liquefiable slopes.

• Constitutive modeling was limited to Mohr–Coulomb and HS Small, excluding more advanced cyclic, anisotropic, or liquefaction-capable models that may provide more realistic soil behavior under strong shaking.

• The numerical analyses were conducted primarily in two dimensions; three-dimensional slope effects were not evaluated.

10.2 Future Research Directions

• Future analyses should incorporate irregular geometries, layered soils, and rock–soil systems to reflect real field conditions more accurately.

• Hydro-mechanical coupling and liquefaction modeling should be included to capture pore pressure buildup, cyclic softening, and post-earthquake delayed failures.

• More advanced constitutive models should be implemented and calibrated using site-specific laboratory data to represent cyclic degradation, anisotropy, and strain-dependent behavior more accurately.

• Extending analyses to three-dimensional slope geometries and real earthquake time histories for improved accuracy.

• Perform field-scale validation using instrumented slopes and compare numerical predictions with observed seismic responses.

11. Conclusions

This study presented a comprehensive comparative assessment of seismic slope stability using both LEM and FEM under pseudo-static and dynamic loading conditions. The results showed that FEM consistently predicts approximately $17 - 19\%$ higher FoS than LEM across all seismic coefficient combinations, reflecting its superior ability to capture stress redistribution, deformation compatibility, and nonlinear soil response. Increasing k_b produced a systematic reduction in FoS, while the inclusion of k_c led to further decreases in stability, with the effect becoming notably significant as k_{bu} approached $0.75 - 1.0kk_h$. Comparison of constitutive models indicated that the Mohr-Coulomb and HS Small models produced closely aligned results, with HS Small yielding slightly lower FoS values by about $1 - 3\%$, attributable to its inclusion of small-strain stiffness and enhanced shear modulus degradation. Mesh refinement had a measurable influence, with fine meshes producing $2 - 7\%$ lower FoS due to improved representation of shear localization and internal stress paths. Evaluation of earthquake loading methods demonstrated that dynamic time-history simulations yielded modestly higher FoS than pseudo-static analyses, whereas idealized harmonic loading produced the lowest FoS, consistent with amplification and resonance tendencies. Overall, the study emphasizes the necessity of incorporating vertical seismic effects, appropriate soil constitutive models, mesh refinement, and realistic dynamic loading to achieve reliable seismic slope stability predictions. These findings offer practical guidance for selecting modeling strategies that better capture true slope behavior under earthquake loading.

Data Availability: The data that support the findings of this study are available from the corresponding author upon reasonable request.

Conflicts of Interest: The authors declare that they have no conflicts of interest.

Funding statement: No funding was received for this research

References

[1] [1] Y. Changwei, Z. Jingyu, L. Jing, Y. Wenying, Z. Jianjing, Slope Seismic Stability, in: Slope Earthquake Stability, Springer, 2016: pp. 163–191.

[2] W. Yiheng, F.M. Nazri, A.M. El-Maissi, S.R. Rahmat, A.M. Kassim, S. Karuppayah, Unlocking seismic slope stability for risk assessment, MethodsX 14 (2025) 103108.

[3] R. Shurpali, L. Govindaraju, PERFORMANCE OF SLOPE UNDER SEISMIC CONDITIONS, (2014).

[4] M.A. Hossain, M.A. Mukit, M.G. Kibria, Investigation of Stability of a Slope Subjected to Water Table and Seismic Load, Int J Comput Appl 140 (2016).

[5] S. Park, W. Kim, J. Lee, Y. Baek, Case study on slope stability changes caused by earthquakes—focusing on Gyeongju 5.8 ML EQ, Sustainability 10 (2018) 3441.

[6] S. Cui, X. Pei, H. Yang, L. Zhu, Y. Jiang, C. Zhu, T. Jiang, R. Huang, Bedding slope damage accumulation induced by multiple earthquakes, Soil Dynamics and Earthquake Engineering 173 (2023) 108157.
[7] Y. Zhang, Earthquake-induced landslides, Springer Singapore, Singapore 10 (2018) 978–981.
[8] S.A. Bastani, B.L. Kutter, SIMULATION OF POST EARTHQUAKE EMBANKMENT FAILURE BY SEEPAGE-INDUCED LIQUEFACTION, (2007).
[9] S. Huang, Y. Peng, Seismic stability analysis of saturated and unsaturated soil slopes using permanent displacement, Advances in Civil Engineering 2018 (2018) 1786392.
[10] Y. Yang, H. Xing, X. Yang, K. Huang, J. Zhou, Two-dimensional stability analysis of a soil slope using the finite element method and the limit equilibrium principle, The IES Journal Part A: Civil Structural Engineering 8 (2015) 251–264.
[11] D. Loukidis, P. Bandini, R. Salgado, Stability of seismically loaded slopes using limit analysis, Geotechnique 53 (2003) 463–479.
[12] M.I. Khan, S. Wang, Comparative study of slope stability of a highway constructed in hilly area using limit equilibrium and finite element methods, in: IOP Conf Ser Earth Environ Sci, 2020: p. 22023.
[13] A. Burman, S.P. Acharya, R.R. Sahay, D. Maity, others, A comparative study of slope stability analysis using traditional limit equilibrium method and finite element method, (2015).
[14] K. Baba, L. Bahi, L. Ouadif, A. Akhssas, Slope stability evaluations by limit equilibrium and finite element methods applied to a railway in the Moroccan Rif, Open Journal of Civil Engineering 2 (2012) 27–32.
[15] J. Zhou, C. Qin, Finite-element upper-bound analysis of seismic slope stability considering pseudo-dynamic approach, Comput Geotech 122 (2020) 103530.
[16] K. Terzaghi, Mechanism of landslides, (1950).
[17] M.A. Mohammad Anis, S.M.A. Jawaid, A review of seismic stability of soil slope., (2016).
[18] A.-J. Li, A. V Lyamin, R.S. Merifield, Seismic rock slope stability charts based on limit analysis methods, Comput Geotech 36 (2009) 135–148.
[19] T. Bao, B. Xu, X. Zheng, Hybrid method of limit equilibrium and finite element internal force for analysis of arch dam stability against sliding, Sci China Technol Sci 54 (2011) 793–798.
[20] T. Kadakci Koca, M.Y. Koca, Comparative analyses of finite element and limit-equilibrium methods for heavily fractured rock slopes, Journal of Earth System Science 129 (2020) 49.
[21] I. Indrawan, A.B. Murti, R. Alfrianto, others, Comparison of stability analysis methods for safe design of volcanic rock slope., Journal of Degraded Mining Lands Management 12 (2024).
[22] K.-C. San, D. Leshchinsky, Seismic slope stability analysis: pseudo-static generalized method, Soils and Foundations 34 (1994) 73–77.
[23] H.B. Seed, R.N. Hwang, J. Lysmer, Soil-structure interaction analyses for seismic response, Journal of the Geotechnical Engineering Division 101 (1975) 439–457.
[24] B.H. Seed, K.L. Lee, I.M. Idriss, Analysis of Sheffield dam failure, Journal of the Soil Mechanics and Foundations Division 95 (1969) 1453–1490.
[25] W.F. Marcuson, A.G. Franklin, P.F. Hadala, Liquefaction potential of dams and foundations, US Army Engineer Waterways Experiment Station, Soils and Pavements Laboratory, 1977.
[26] T. Akhlaghi, M. Neishapouri, A study on the pseudostatic analysis of the upper San Fernando dam using FE simulations and observed deformations during the 1971 earthquake, in: Fourth International Conference on Earthquake Geotechnical Engineering, 2007: pp. 1–12.
[27] D. Choudhury, S. Basu, J.D. Bray, Behaviour of slopes under static and seismic conditions by limit equilibrium method, in: Embankments, Dams, and Slopes: Lessons from the New Orleans Levee Failures and Other Current Issues, 2007: pp. 1–10.
[28] H. Gullu, H. Canakci, R. Iyisan, A Study About Effect Of Soil Model On Slope Under Vibration Load, in: 2013.

[29] M. Liu, Y. Gao, H. Liu, A nonlinear Drucker–Prager and Matsuoka–Nakai unified failure criterion for geomaterials with separated stress invariants, International Journal of Rock Mechanics and Mining Sciences 50 (2012) 1–10.
[30] X. Tan, J. Wang, Finite element reliability analysis of slope stability, Journal of Zhejiang University-SCIENCE A 10 (2009) 645–652.
[31] .S. Shadkam, .. Bessimbayev, U.. Begaliev, S.. Niyetbay, THE COMPARISON OF DEFORMATION CALCULATION RESULTS OF STRUCTURES UNDER SEISMIC IMPACT USING MOHR-COULOMB AND HARDENING SOIL SMALL (HSS) SOIL MODELS, (2024).
[32] M. Saleh Asheghabadi, X. Cheng, Analysis of undrained seismic behavior of shallow tunnels in soft clay using nonlinear kinematic hardening model, Applied Sciences 10 (2020) 2834.
[33] D. Liu, X. Chen, Shearing characteristics of slip zone soils and strain localization analysis of a landslide, Geomechanics Engineering 8 (2015) 33–52.
[34] L. Deghoul, S. Gabi, A. Hamrouni, The influence of the soil constitutive models on the seismic analysis of pile-supported wharf structures with batter piles in cut-slope rock dike, Studia Geotechnica et Mechanica 42 (2020).
[35] Z. Ma, H. Liao, F. Dang, Y. Cheng, Seismic slope stability and failure process analysis using explicit finite element method, Bulletin of Engineering Geology and the Environment 80 (2021) 1287–1301.
[36] L. Yanhong, G. Zeng, J. Haibin, L. Hongqiang, D. Quancai, Failure effect of seismic faults and the slope stability along highways under seismic hazards based on dynamic finite element analysis and genetic algorithm, Geotechnical and Geological Engineering 39 (2021) 5191–5200.
[37] A.S. Jacob, K. Venkataramana, Slope Stability Analysis Under Earthquake Load Using Plaxis Software, Journal of Advances in Geotechnical Engineering 3 (2021) 1–8.
[38] R.B.J. Brinkgreve, E. Engin, H.K. Engin, Validation of empirical formulas to derive model parameters for sands, Numerical Methods in Geotechnical Engineering 137 (2010) 142.
[39] B. der Kwaak, Modelling of dynamic pile behaviour during an earthquake using PLAXIS 2D: Embedded beam (row), Master of Science Thesis (2015).
[40] A. Zewdu, Modeling the slope of embankment dam during static and dynamic stability analysis: a case study of Koga dam, Ethiopia, Model Earth Syst Environ 6 (2020) 1963–1979.
[41] H.B. Seed, Considerations in the earthquake-resistant design of earth and rockfill dams, Geotechnique 29 (1979) 215–263.
[42] S.L. Kramer, J.P. Stewart, Geotechnical earthquake engineering, CRC Press, 2024.
[43] H.B. Seed, Design of gravity retaining structures for dynamic loads, in: Proc. of Specialty Conference on Lateral Stresses in the Ground and Design of Earth Retaining Structures, 1970: pp. 103–147.
[44] F.I. Makdisi, H.B. Seed, Simplified procedure for estimating dam and embankment earthquake-induced deformations, Journal of the Geotechnical Engineering Division 104 (1978) 849–867.
[45] C. Deepankar, S.S. Nimbalkar, Pseudo-dynamic approach of seismic active earth pressure behind retaining wall, Geotechnical and Geological Engineering 24 (2006).
[46] X. Yang, E. Zhai, Y. Wang, Z. Hu, A comparative study of pseudo-static slope stability analysis using different design codes, Water Science and Engineering 11 (2018) 310–317.
[47] C. Schmüdderich, Contributions to the stability assessment of slopes subjected to seismic loading, Ruhr-Universität Bochum, 2024.
[48] S.Y. Liu, L.T. Shao, H.J. Li, Slope stability analysis using the limit equilibrium method and two finite element methods, Comput Geotech 63 (2015) 291–298.
[49] C.A. Siregar, H.R. Nuggraha, G.A. Azhar, D. Warlina, Slope Stability Analysis Using Plaxis Slope/W (Case Study: Bagbagan-Jampangkulon Road Section STA 8+ 400, STA 8+ 200, and STA 13+ 000), in: IOP Conf Ser Earth Environ Sci, 2024: p. 12031.

[50] R.B.J. Brinkgreve, W. Broere, D. Waterman, R. Al-Khoury, K. Bakker, P. Bonnier, H. Burd, G. Soltys, P. Vermeer, D. Den Haag, 2D–Version 8, Delft, Delft University of Tehnology PLAXIS Bv 18 (2004).
[51] T. Das, V. Dilli Rao, D. Choudhury, Seismic stability and deformation analysis of a south India hill slope by finite elements, Nat Hazards Rev 24 (2023) 4022050.
[52] N.M. Saima, A. Kasab, Effect of mesh coarseness on slope stability analysis using 2D and 3D finite element method, Jurnal Kejuruteraan 36 (2024) 497–507.
[53] H.-D. Lin, W.-C. Wang, A.-J. Li, Investigation of dilatancy angle effects on slope stability using the 3D finite element method strength reduction technique, Comput Geotech 118 (2020) 103295.
[54] M.M. Sazzad, S. Roy, N.A. Biman, Effect of Earthquake on the Stability of Slope by Pseudo-Static and Dynamic Approach, (2021).
[55] A. Eikebrokk, A.M. Kaynia, Nonlinear finite element analyses of earthquake effects in slopes, in: Geotechnical Engineering Challenges to Meet Current and Emerging Needs of Society, CRC Press, 2024: pp. 1109–1112.
[56] S. Ismail, F.H. Chehade, R. Al Wardany, Slope stability analysis under seismic loading, in: Second Europian Conference on Earthquake Engineering and Siesmology, 2014: pp. 25–29.